





Nonstationary Resonant Oscillations of a Gyroscopic Rigid Rotor with Nonlinear Damping and Non-ideal Energy Source

Zharilkassin Iskakov^(✉) , Nutulla Jamalov , and Azizbek Abduraimov 

Institute of Mechanics and Engineering, Al-Farabi Kazakh National University, Almaty, Kazakhstan

Abstract. The article is concerned with the effect of nonlinear cubic damping of an elastic support on unsteady resonant vibrations of a gyroscopic rigid rotor when interacting with a non-ideal energy source. It is confirmed that nonlinear cubic damping can suppress not only the maximum amplitude, but also the amplitude of unsteady oscillations behind the rotation speed corresponding to the amplitude peak. It shifts the control parameter corresponding to the maximum amplitude, downward with a rigid nonlinear elastic characteristic of the support material, and upward with a soft nonlinear elastic characteristic of the support material. An increase in the nonlinear cubic damping coefficient can significantly weaken the Sommerfeld effect with a nonlinear jump in unsteady oscillations, up to its complete elimination. The difference in the values of the maximum amplitude and in the corresponding values of the control parameter in the resonance curves with an increasing and decreasing control parameter is explained by the difference in the values of the same parameters relating to the jumping effects during the acceleration and runout of the rotary machine.

Keywords: Gyroscopic rotor · Non-ideal source · Nonlinear damping · Nonstationary oscillation

1 Introduction

Vibration is commonly found in rotating equipment during start-up, operation, and shutdown.

It is very important to use properties and characteristics of the material of the supports for attenuation and damping of vibration in order to stabilize movement of an unbalanced rotor and vibration systems.

A convenient way to introduce attenuation to support bearings in a rotor system on viscoelastic flexible rubber supports [1]. In parallel with the development of viscoelastic material modeling, which helps to describe the complexity of material properties, the use of viscoelastic components in the dynamics of the rotor and vibration systems also increased as a whole, in particular with non-linear elastic characteristic and damping. So, for example, in works [2–5], the research results show that linear and nonlinear cubic damping can significantly suppress the maximum amplitudes, eliminate the jump-like

phenomena of a nonlinear system. In nonresonant regions, where the vibration frequency is higher than its resonant value, nonlinear cubic damping, unlike linear damping, can reduce the amplitude of the rotor vibration. Therefore, in all regions of oscillation frequency (rotation speed), only non-linear cubic damping can support the performance characteristics of the vibration isolator. [2] provides an excellent overview of research on passive vibration isolation systems.

In work [6], a nonlinear damping suspension can affect the stability of a flexible rotor in short support bearings, a numerical method is used to solve the equations of motion, and bifurcation diagrams, orbits, Poincaré maps, and amplitude spectra are used to display motions. The results of works [2–5] are confirmed.

In this paper, a gyroscopic nonlinear rotor system is considered on the assumption that it receives an action from an energy source with a limited power. Movement of the oscillatory system under the influence of such sources is accompanied by mutual influence on each other: the energy source and the oscillatory system. Interaction of an oscillatory system with an energy source should also manifest itself in non-stationary modes of motion, especially in such practically important cases as the case of passage of oscillatory systems through resonance.

The process of passage of an oscillatory system through resonance, taking into account its interaction with an energy source, was considered in [7, 8] and in other works. A complete review of articles on research concerning basic properties of vibrational non-ideal systems is given in work [9]. In particular, it has been found that under conditions when the power reserve of the energy source is small, the course of the process depends very much on the characteristics of the energy source. Changes in the frequency of vibrations are closely related to changes in the amplitude of vibrations. In the region of large amplitudes, the rate of passage of the system through the resonance sharply slows down; as the amplitude decreases, the rate of passage increases, if the excess power of the energy source is sufficient for this (a typical Sommerfeld effect). Such resonance capture can cause failure of the rotor shaft, bearings and other structural parts. Therefore, vibration isolation is very important for movement stabilization, and specifically with the help of complex linear and non-linear cubic damping of the elastic support, taking into account change in voltage supplied to the motor during acceleration and runout.

2 Equations of Motion

The following system is considered: gyroscopic rotor – elastic support – DC motor, the structural diagram of which is shown in Fig. 1. The rotor consists of a shaft with a length L , mounted vertically by means of a lower hinge and an upper elastic support spaced from it at a distance l_0 and a disk fixed at the free end of the shaft, having a mass m , a polar moment of inertia I_p and a transverse moment of inertia I_T , the same for any direction. With such an arrangement of the shaft with the disk relative to the supports and with a sufficiently high rotation speed of the shaft $\dot{\varphi}$, the rotor can be considered as a gyroscope. The elastic support has linear stiffness c_1 , non-linear stiffness c_3 , linear damping μ_{d1} and non-linear cubic damping μ_{d3} . The position of the geometric center of the disk S is determined by coordinates x, y in a fixed coordinate system $Oxyz$, and the

position of the shaft and the rotor as a whole in space by the Euler angles α , β and the angle of rotation φ . The angles α , β are small, consequently, the movement of the rotor in the direction of the coordinate axis z is neglected. Next, denote the coordinates of the center of mass m of the disk through x_m and y_m . Assume also that the linear eccentricity e lies in the direction of the N axis of the $ONKZ$ coordinate system. Restrict to small deviations of the rotor axis. Then $\sin\alpha \approx \alpha$, $\sin\beta \approx \beta$, $\cos\alpha \approx 1$, $\cos\beta \approx 1$.

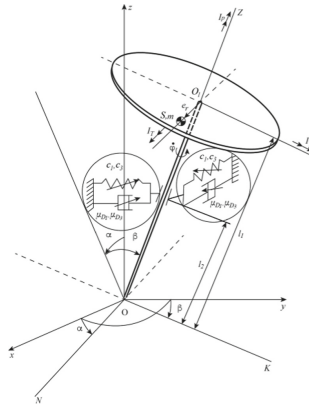


Fig. 1. Rotor geometry.

Express the projections of the angular velocity of the rotor in the coordinate axes of the $ONKZ$ system, the coordinates of the center of mass of the disk and the coordinates of the upper support through the angular coordinates α , β and φ , and find expressions for determination of the kinetic energy, the potential energy of the rotor, the Rayleigh function and the projections of the moments of forces acting on the system and the motor torque with straight characteristic. Substituting them into the Lagrange equations of the second kind, and using the following dimensionless parameters

$$\begin{aligned}
 l &= l_0/L; \bar{l} = l\omega_0; \bar{I}_P = I_P/(mL^2); \bar{I}_T = I_T/(mL^2); \\
 \bar{C}_1 &= c_1/(m\omega_0^2); e_r = e/[L(1 + \bar{I}_T)]; I_{P1} = \bar{I}_P/(1 + \bar{I}_T); \\
 \bar{G} &= g/(L\omega_0^2); C_3 = c_3 l_0^4/[mL^2\omega_0^2(1 + \bar{I}_T)]; \\
 \mu_1 &= \mu_{d1}/[mL^2\omega_0(1 + \bar{I}_T)]; \mu_3 = \mu_{d3}\omega_0/[mL^2(1 + \bar{I}_T)]; \\
 u_1 &= C_M \Phi\omega_0 U/[RmL^2(1 + \bar{I}_T)]; u_2 = (C_M C_E \Phi^2/R + q_m)/[mL^2\omega_0(1 + \bar{I}_T)],
 \end{aligned}
 \tag{1}$$

where $\omega_0 = \sqrt{(k_1 l_0^2 - mgL)/[mL^2 - (I_P - I_T)]}$ the natural frequency of the damped rotor system, $C_M = C_E$ is the mechanical (or electrical) constant, Φ is the magnetic flux of one pole, U is the voltage drop across the entire power circuit of the motor with resistance R , q_m is the coefficient of resistance to the rotation of the motor rotor, obtain

the equations of the rotor motion in the form

$$\begin{aligned} \alpha'' + \omega_n^2 \alpha &= e_r \varphi'^2 \cos \varphi - I_{P1} \varphi' \beta' - \mu_1 \alpha' - \mu_3 \alpha'^3 - C_3 \alpha^3, \\ \beta'' + \omega_n^2 \beta &= e_r \varphi'^2 \sin \varphi + I_{P1} \varphi' \alpha' - \mu_1 \beta' - \mu_3 \beta'^3 - C_3 \beta^3, \\ \varphi'' &= [e_r (\alpha'' \sin \varphi - \beta'' \cos \varphi) - I_{P1} (\alpha'' \beta + \alpha' \beta')] + u_1 - u_2 \varphi' / I_{P1}, \end{aligned} \tag{2}$$

where $\omega_n = \sqrt{(\bar{K}_1 l^2 - \bar{G}) / (1 + \bar{I}_T)}$ the dimensionless natural frequency of the linear rotor system (2) at $\bar{I}_T \gg \bar{I}_P$, u_1 is the control parameter (controlling parameter), depending on the voltage on the motor; u_2 - a parameter that depends on the type of energy source.

On the right-hand part of the system of Eqs. (2) perturbations containing φ'' , were discarded, since in the region close to the resonance velocity $\varphi'' \ll \varphi'^2$, and perturbations having a parameter \bar{I}_P (in what follows, assuming that $\bar{I}_P \ll \bar{I}_T$) and values of the second and higher orders of smallness with respect to α, β , their derivatives, and their combinations. The indicated disturbances are small in comparison with disturbances, the amplitudes of which are proportional to the angular velocity squared.

Equations (2) are a system of second order nonlinear ordinary differential equations with respect to α, β and φ .

3 Solutions of Motion Equations

Consider a rotor system close to a linear system. To use the Bogolyubov method, the following restrictions are taken to solve Eqs. (2). The projections of the moments of the damping forces $\mu_1 \alpha', \mu_1 \beta'$ and $\mu_3 \alpha'^3, \mu_3 \beta'^3$, as well as the moment of the cubic component of the restoring force $C_3 \alpha^3, C_3 \beta^3$, the moments of the centrifugal force of the imbalance $e_r \varphi'^2 \cos \varphi, e_r \varphi'^2 \sin \varphi$ of mass and are considered small in comparison with the projections of the moments of the vibration inertia force and the linear restoring force acting in the system. Assuming that $\bar{I}_P \ll \bar{I}_T$ the projections of the moment of the passive gyroscopic force can also be considered small $I_{P1} \varphi' \alpha', I_{P1} \varphi' \beta'$, limit also to considering a spinning rotor: $\varphi'^2 \gg \bar{G}$ and motion in the resonance range, where the frequency of free oscillations ω_n is close to the frequency of forced oscillations Ψ . Therefore, search for solutions (2) in the form:

$$\alpha = A \cos(\varphi + \chi), \beta = A \sin(\varphi + \chi). \tag{3}$$

Here variables A, χ, Ψ will be slowly changing functions of times \bar{t} . They represent the most essential parameters of motion: A - vibration amplitude, χ - phase shift angle between the angular coordinate α or β and the disturbing moment.

Following Bogolyubov’s method, obtain a system of equations in relation to A, χ, Ψ , the approximate solutions of which can be represented in the form

$$\Psi = \Omega + \varepsilon E_1(\bar{t}, \Omega, a, \xi), A = a + \varepsilon E_2(\bar{t}, \Omega, a, \xi), \chi = \xi + \varepsilon E_3(\bar{t}, \Omega, a, \xi), \tag{4}$$

where $\varepsilon E_1(\bar{t}, \Omega, a, \xi), \varepsilon E_2(\bar{t}, \Omega, a, \xi), \varepsilon E_3(\bar{t}, \Omega, a, \xi)$ are small periodic functions of time $\bar{t}, \varepsilon \ll 1$ is the small parameter.

After averaging of the obtained equations of motion, which are equivalent to the system (2), obtain the system of equations for the transient process of the rotor in the following form

$$\begin{aligned} d\Omega/d\bar{t} &= (u_1 - u_2\Omega + e_r a \omega_n \Omega \sin \xi)/I_{P1}, \\ da/d\bar{t} &= -(e_r \Omega^2 \sin \xi / \omega_n + \mu_1 a + 3\mu_3 \omega_n^2 a^3 / 4)/2, \\ d\xi/d\bar{t} &= \omega_n - \Omega - e_r \Omega^2 \cos \xi / (2\omega_n a) + 3C_3 a^2 / (8\omega_n), \\ d\varphi/d\bar{t} &= \Omega. \end{aligned} \quad (5)$$

4 Unsteady Oscillations

The system of equations for the unsteady process (5) was modeled in the Matlab-Simulink package. The control parameter u_1 “slowly” increased uniformly ($\nu > 0$) and “slowly” decreased uniformly over ($\nu < 0$) time in accordance with the regularity $u_1 = u_{10} + \nu \bar{t}$ [10].

The general parameters of the system have been selected in accordance with various design parameters of the centrifuge used in [5] for experimental studies, and have the following dimensionless values: $e_r = 0.0346$, $\omega_n \approx 1$, $I_{P1} = 0.021$ ($\bar{I}_P = 0.026$, $\bar{I}_T = 0.213$). The values of the parameters C_3 , μ_1 , μ_3 , u_1 , u_2 and ν were chosen in the course of numerical experiments, and the values of μ_1 and μ_3 , taking into account those values at which the jumping effects disappear, in accordance with the rest of the known design parameters necessary for creation of the effective vibration isolation for the centrifuge based on gyroscopic rotor. The values of the parameters for the initial conditions are borrowed from the frequency characteristics of the stationary oscillation at $\Omega_0 < \omega_n$ and $\Omega_0 > \omega_n$. Thus, for the parameters $u_2 = 1.245$, $\mu_1 = 0.01$ and $\mu_3 = 0.01, 0.02$, we take the following initial conditions: at $C_3 = 0.1$ for the case $\nu = 0.00025$: $\bar{t} = 0$, $\Omega_0 = 0.88$, $u_{10} = 1.096$, $a_0 = 0.11$, $\xi_0 = -0.0420$, for the case $\nu = -0.00025$: $\bar{t} = 0$, $\Omega_0 = 1.2$, $u_{10} = 1.50$, $a_0 = 0.12$, $\xi_0 = 0.0253$; for $C_3 = -0.1$ for the case $\nu = 0.00025$: $\bar{t} = 0$, $\Omega_0 = 0.88$, $u_{10} = 1.096$, $a_0 = 0.112$, $\xi_0 = -0.0424$, for the case $\nu = -0.00025$: $\bar{t} = 0$, $\Omega_0 = 1.2$, $u_{10} = 1.494$, $a_0 = 0.124$, $\xi_0 = 0.0253$.

The abscissa axis has two scales: the parameter scale u_1 and the corresponding time scale \bar{t} .

The graphs of dependence $a = a(u_1)$ non-stationary oscillations of the rotor, built according to the results of modeling Eq. (5), are shown in Figs. 2 and 3.

From these figures, first of all, the damping effect of the parameter μ_3 on the maximum value a_m and on the quasiperiodic variation of the oscillation amplitude behind the amplitude peak and the influence μ_3 on the value of the control parameter u_m corresponding to the maximum amplitude are obvious. Non-linear cubic damping shifts the control parameter u_m (shaft speed Ω_m) corresponding to the maximum amplitude at $C_3 > 0$ (Fig. 2a) downwards, and at $C_3 < 0$ (Fig. 3b) upwards, i.e. in both cases, the characteristics of the nonlinear stiffness of the support Ω_m approaches ω_n .

The values of the maximum amplitude and the corresponding control parameter in the resonance curves during acceleration (Figs. 2a and 3a) and runout (Figs. 2b and 3b) of the rotary machine, approximately determine the positions of the jumping effects. As

the nonlinear cubic damping coefficient increases, the distance between these positions decreases, and its further increase can completely eliminate the jumping phenomena.

Thus, increasing the value of nonlinear cubic damping can significantly weaken the Sommerfeld effect with a nonlinear jump, up to its complete elimination.

The change in the characteristics of the nonlinear stiffness of the elastic support and the nature of the change in the controlling parameter significantly affects the description of the dependency graphs $a = a(u_1)$.

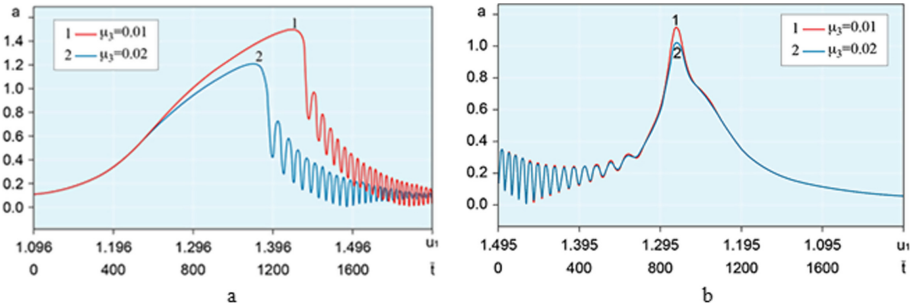


Fig. 2. Transition through resonance in the case of $C_3 = 0.1$ with different values of μ_3 and angular acceleration: a - $\nu = 0.00025$, b - $\nu = -0.00025$.

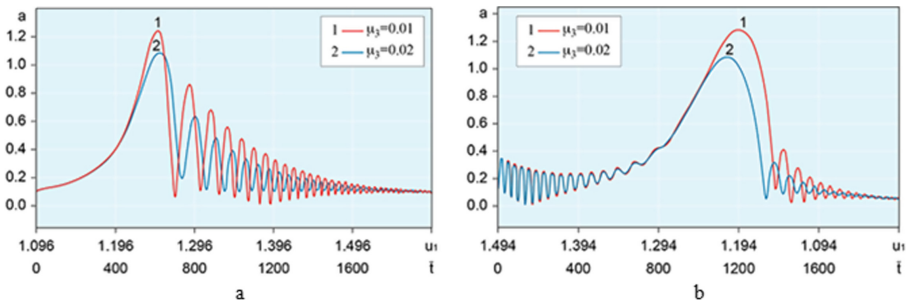


Fig. 3. Transition through resonance in the case of $C_3 = -1$ with different values of μ_3 and angular acceleration: a - $\nu = 0.00025$, b - $\nu = -0.00025$.

The difference in the values of the maximum amplitude, the values of the corresponding control parameter (shaft rotation speed), with increasing (Figs. 2a and/or 3a) and decreasing (Figs. 2b and/or 3b) control parameter is explained by jumping transitions with different values of these parameters during the take-off and runout of the rotary machine. In the case with $C_3 > 0$ and with $\nu > 0$ the jump is carried out from a higher amplitude to a lower one (Fig. 2a), with a $\nu < 0$ from a lower amplitude to a higher one (Fig. 2b), and with $C_3 < 0$ vice versa (Figs. 3b and 3a, respectively). This is usually observed in experimental studies during acceleration and deceleration of the machine [5]. With a rigid nonlinear characteristic of elasticity, the support $C_3 > 0$ jumps will be located in the area of the shaft rotation speed, where $\Omega > \omega_n$ (Fig. 2), with the soft

nonlinear elasticity characteristic of the support $C_3 < 0$ - in the range of shaft rotation speed, where $\Omega < \omega_n$ (Fig. 3).

After the transition of the amplitude peak with a slow change in the control parameter, the response amplitude of the system, having made damped oscillations, tends to certain values, regardless of the values of the nonlinear cubic damping coefficient.

To confirm the analytical study, the system of Eq. (2) was solved directly numerically. Figure 4 shows the numerical results for passage through resonance with a rigid nonlinear elastic characteristic of the support of the support material and a “slowly” increasing value of the control parameter u_1 . In this figure, the effects of damping by the parameter μ_3 of resonant oscillations are also observed after resonant damped beats. Damped beats occur due to the superposition of forced non-stationary oscillations and damped natural oscillations with frequencies closely matching in the vicinity of the resonance [11]. The results in Fig. 4 are consistent with previous analytical results shown in Figs. 2a and 3a. The differences are in the value of the maximum vibration amplitude and the offset of the corresponding value of the control parameter. Despite this, the basic behavior of the transient process persists.

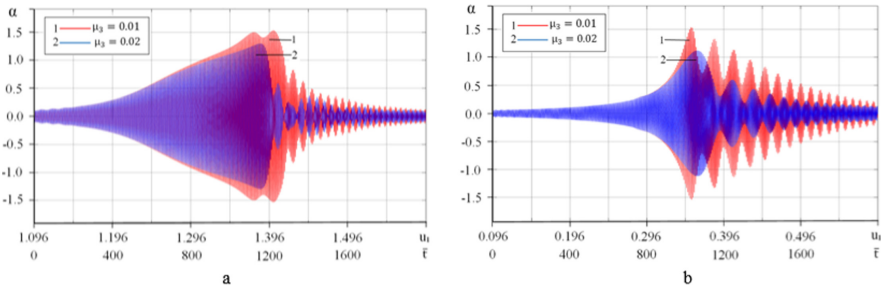


Fig. 4. Passage through resonance $c \nu = 0.00025$ according to the results of the numerical solution of Eqs. (2) for a - $C_3 = 0.1$, b - $C_3 = -0.1$.

To ensure the reliability of the process of transition through resonance, from Eq. (2), setting equal to zero the expression $e\Omega^2$ due to the moment of inertia of the mass unbalance and the damping coefficients μ_1 and μ_3 , the equation of the reference line of the resonance curve will be obtained:

$$\Omega = \omega_n + \frac{3C_3 a^2}{8\omega_n}, \tag{6}$$

Assuming that, $\nu \ll \Omega^2$ the maximum amplitudes and the corresponding rotational speeds of the resonance curves approximately satisfy Eq. (6). So, for example, at the $C_3 = 0.1, \nu = 0.00025, \mu_1 = 0.01, \mu_3 = 0.01, 0.02$ maximum amplitude = 1.507, 1.20715, the rotation speed corresponds $\Omega = 1.085, 1.040$, respectively (Fig. 2a), at $C_3 = -0.1, \nu = 0.00025, \mu_1 = 0.01, \mu_3 = 0.01, 0.02$ maximum amplitude $a = 1.316, 1.10792$ - the rotation speed $\Omega = 0.935, 0.954$, respectively (Fig. 3b).

5 Conclusions

Differential equations of motion of a gyroscopic rigid unbalanced rotor with nonlinear cubic damping, a non-ideal energy source are constructed and solved by the Bogolyubov method. Differential equations of unsteady oscillations of the rotor are obtained, which were solved numerically for the transient process through the resonance region.

It is shown that nonlinear cubic damping significantly suppresses the maximum amplitude, and the amplitude of unsteady oscillations after the value of the control parameter corresponding to the amplitude peak. It shifts this control parameter value downwards with the rigid non-linear elastic characteristic ($C_3 > 0$) of the support material and upwards with the soft non-linear elastic characteristic ($C_3 < 0$) of the support material.

Nonlinear cubic damping can significantly weaken the Sommerfeld jumping effect, up to its complete elimination.

The values of the maximum amplitude and the corresponding control parameter in the resonance curves with an increasing and decreasing control parameter approximately correspond to the values of the oscillation amplitude and the control parameter related to jumping effects during acceleration and runout of a rotary machine.

There is an agreement between the results of analytical solutions and numerical solutions of the equations of rotor motion.

The research results can be used in the manufacture of a vibration isolator, which significantly suppresses the peak amplitude, and the amplitude of oscillations behind the resonant rotation speed, for a vibrating system, incl. rotary one.

Acknowledgments. This research is funded by the the Ministry of Education and Science of the Republic of Kazakhstan (Grant No. AP08856763).

References

1. Zakaria, A.A., Rustighi, E., Ferguson, NS: A numerical investigation into the effect of the supports on the vibration of rotating shafts. In: Proceedings of the 11-th International Conference on Engineering Vibration, Ljubljana, Slovenia, pp. 539–552 (2015)
2. Peng, Z.K., Meng Lang, Z.Q., Zhang, W.M., Chu, F.L.: Study of the effects of cubic non-linear damping on vibration isolations using harmonic balance method. *Int. J. Nonlin. Mech.* **47**(10), 1065–1166 (2012)
3. Ho, C., Lang, Z., Billings, S.A.: The benefits of non-linear cubic viscous damping on the force transmissibility of a Duffing-type vibration isolator. In: Proceedings of UKACC International Conference on Control, UK, Cardiff, UK, pp. 479–484 (2012)
4. Zhenlong, X., Xingjian, J., Li, C.: The transmissibility of vibration isolators with cubic non-linear damping under both force and base excitations. *J. Sound. Vib.* **332**(5), 1335–1354 (2013)
5. Iskakov, Z., Bissebayev, K.: The nonlinear vibrations of a vertical hard gyroscopic rotor with nonlinear characteristics. *Mech. Sci.* **10**, 529–544 (2019)
6. Yan, S., Dowell, E.H., Lin, B.: Effects of nonlinear damping suspension on nonperiodic motions of a flexible rotor in journal bearings. *Nonlinear. Dyn.* **78**(2), 1435–1450 (2014)

7. Dimentberg, M.F., McGovern, L., Norton, R.L., Chapdelaine, J., Harrison, R.: Dynamics of an unbalanced shaft interacting with a limited power supply. *Nonlinear Dyn.* **13**(2), 171–187 (1997)
8. Samantaray, A.K., Dasgupta, S.S., Bhattacharyya, R.: Sommerfeld effect in rotationally symmetric planar dynamical systems. *Int. J. Eng. Sci.* **48**(1), 21–36 (2010)
9. Cvetićanin, L.: Dynamics of the non-ideal mechanical systems, a review. *J. Serbian Soc. Comput. Mech.* **4**(2), 75–86 (2010)
10. Warminski, J.: Regular and chaotic vibrations of Van der Pol-Mathieu oscillator with non-ideal energy source. *J. Theor. Appl. Mech.* **2**(40), 415–433 (2002)
11. Grobov, V.A.: *Asymptotic Methods for Calculating Bending Vibrations of Turbomachine Shafts*. Publishing house of the Academy of Science, USSR, Moscow (1961)